

# Benchtop $^1\text{H}$ NMR Study of Hyperpolarized Charged and Neutral Ir-IMes Dihydride Complexes

Raphael Kircher, Jingyan Xu, Erik van Dyke, Rozana Mazlumian, Dmitry Budker, and Danila A. Barskiy\*



Cite This: *Organometallics* 2025, 44, 1251–1256



Read Online

ACCESS |



Metrics & More

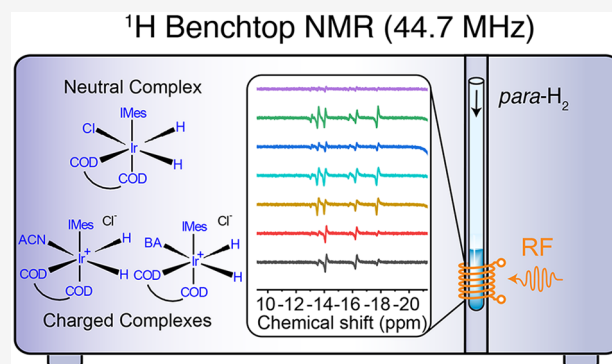


Article Recommendations



Supporting Information

**ABSTRACT:** In this work, we utilize  $^1\text{H}$  benchtop nuclear magnetic resonance (NMR) spectroscopy (proton frequency 44.7 MHz) for real-time monitoring of spin-transfer catalysis, starting from an iridium-based organometallic precursor complex  $[\text{Ir}(\text{IMes})(\text{COD})\text{Cl}]$  (IMes = 1,3-bis(2,4,6-trimethylphenyl)imidazol-2-ylidene, COD = cyclooctadiene) with hydrogen in solution. We identify two distinct activation pathways: first, via the formation of a neutral intermediate complex  $[\text{Ir}(\text{IMes})(\text{COD})(\text{H})_2\text{Cl}]$ , and second, via the formation of charged complexes  $[\text{Ir}^+(\text{IMes})(\text{COD})(\text{H})_2\text{R}]\text{Cl}^-$  (with R being bound ligands: acetonitrile, ammonia, or benzylamine). We conclude that the pathway direction is dominated by solvent polarity and explore SABRE (Signal Amplification by Reversible Exchange) of an acetonitrile solvent in the presence of a benzylamine coligand. These results are important for a better understanding of chemical dynamics in SABRE systems as well as for the fundamental physics experiments that require stable and long-lasting polarization of highly concentrated molecules (e.g., those from the solvent itself).



## INTRODUCTION

Weak signals remain a significant challenge for analytical applications of NMR spectroscopy due to the inherently low thermal equilibrium spin polarization of samples. This is especially true for benchtop NMR spectrometers with limited available magnetic field strengths.<sup>1–4</sup> Despite these limitations, benchtop NMR spectrometers offer unique advantages,<sup>5–7</sup> such as affordability and accessibility, which makes them promising tools for studying organometallic complexes and advancing our understanding of their chemistry and catalysis.

Complexes of iridium find applications in various fields of catalysis,<sup>8–11</sup> one special application is magnetization transfer catalysis in the process termed SABRE (signal amplification by reversible exchange).<sup>12–17</sup> In SABRE, the nuclear spin order of parahydrogen ( $p\text{H}_2$ ) is transferred to magnetization of exchanging target molecules that can lead to an increase in polarization, and, thus, to an enhancement of NMR signals by several orders of magnitude. Hyperpolarization techniques are particularly suitable in combination with benchtop NMR spectrometers.<sup>18–20</sup> In SABRE, polarization transfer is facilitated through a scalar coupling network between hydrides and nuclei in ligated target molecules that bind to the same polarization transfer catalyst (PTC).<sup>21–23</sup>

The activation (i.e., a chemical transformation process for obtaining the active form of the PTC) of a common SABRE catalyst precursor  $[\text{Ir}(\text{IMes})(\text{COD})\text{Cl}]$  plays a critical role in determining the overall efficiency of SABRE. During the activation, the catalyst undergoes key transformations—e.g., hydrogenation of COD (cyclooctadiene) to COE (cyclo-

octene) and COA (cyclooctane)—and multiple ligand exchange reactions that directly influence the nature of the formed PTCs. Optimizing the activation process (i.e., finding optimal concentrations of the participating chemicals) ensures that the most “effective” PTCs will participate in the subsequent hyperpolarization steps.

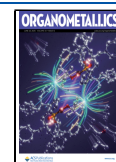
Because of its ability to reversibly bind chlorine, active PTCs as well as intermediate Ir-dihydride complexes of the activation process can exist in charged and neutral forms.<sup>24–26</sup> Charged complexes are those that have a chlorine anion displaced in the coordination sphere by a ligated substrate and the neutral ones have a chlorine in the coordination sphere. In neutral PTCs, the chemical shift difference between two hydride spins facilitates equilibration between ortho- and parahydrogen at high fields,<sup>25</sup> while in the charged complexes the two hydride spins are chemically equivalent, preserving parahydrogen state unless optimal SABRE conditions are fulfilled. In most of the SABRE literature, only the symmetric charged complex is typically presented as the dominant PTC and other possible PTCs are not considered. Mewis et al. have presented structures of mixed charged PTCs in methanol with

**Received:** February 10, 2025

**Revised:** May 22, 2025

**Accepted:** May 23, 2025

**Published:** June 9, 2025



acetonitrile and pyridine as a coligand (Co-L);<sup>27</sup> DFT calculations were performed to study ligand exchange pathways. Neutral PTCs have been identified by Tickner et al. (including 2D-correlation NMR experiments).<sup>24,26,28</sup>

In this work, we used SABRE to study the activation of an Ir-based N-heterocyclic carbene complex, [Ir(IMes)(COD)Cl] (concentration of 3–5 mM), with hydrogen in various solvents using benchtop <sup>1</sup>H NMR spectroscopy. Ir-dihydride complexes of neutral configurations were found in dichloromethane (DCM), charged Ir-dihydride complexes in methanol (MeOH), and a mix of neutral and charged Ir-dihydride complexes were identified in acetonitrile (ACN) or in multiphase systems (e.g., DCM/water mixtures). We also present solvent-SABRE with acetonitrile, a weakly coordinating substrate that requires a stabilizing Co-L (benzylamine). To the best of our knowledge, acetonitrile was used for the first time as a solvent for SABRE hyperpolarization. Activation of various substrates for SABRE experiments (acetonitrile, ammonia, benzylamine) in different solvents (methanol, dichloromethane, and their mixtures) was monitored and assignments of <sup>1</sup>H benchtop NMR peaks formed during the activation are presented. Better understanding of the chemical processes that take place during the activation allowed us to develop a protocol for achieving stable and reproducible molar polarization of acetonitrile, capable of generating hyperpolarization-enhanced <sup>15</sup>N signals on naturally abundant [<sup>15</sup>N]-ACN molecules.<sup>29,30</sup>

## RESULTS AND DISCUSSION

Catalytic activation of [Ir(COD)(IMes)Cl] (IMes = 1,3-bis(2,4,6-trimethylphenyl)-imidazol-2-ylidene; COD = cyclooctadiene), a common precursor complex of PTCs required for SABRE hyperpolarization, in acetonitrile (ACN) solvent with added benzylamine (BA) (Co-L) is shown in Figure 1A in a time series (30 min monitoring, temporal resolution of 20 s) of <sup>1</sup>H NMR spectra. The gas handling setup used in this work was described previously<sup>23,31</sup> and details are shown in the Supporting Information.

The activation process studied involves hydrogenation of the COD ligand, which is an irreversible process that involves transformation of a square-planar Ir(I)-precursor complex into an octahedral Ir(III)-dihydride complex. The time scale for this activation process is on the order of minutes to hours, depending on substrate, solvent, and temperature. However, in this work, the generation of PTCs required for SABRE with ACN was elucidated and can be observed with enhanced <sup>1</sup>H NMR resonances at around –23 ppm using *p*H<sub>2</sub> bubbling prior to NMR detection and benzylamine as a stabilizing Co-L (Figure 1B). Moreover, generated intermediate Ir-dihydride complexes (I-A, I-B, and I-C, structures shown in Figure 1B) can be detected within a chemical shift range between –12 and –18 ppm; the corresponding assignments are highlighted (note the increased NMR scale in the zoom-in). The assignment was confirmed by comparing spectra acquired under conditions without Co-L addition. Under these conditions, only the generation of I-A and I-B was observed which is discussed in more detail below (see Figure 2).

Intermediate Ir-dihydride complexes, denoted as I-A, I-B, and I-C display characteristic PASADENA patterns,<sup>32,33</sup> originating from the bound hydrides with decreasing respective signal intensity (Figure 1A). The fact that two multiplets are distinguishable allows to conclude that complexes have an asymmetric configuration with one hydrogen being trans to the

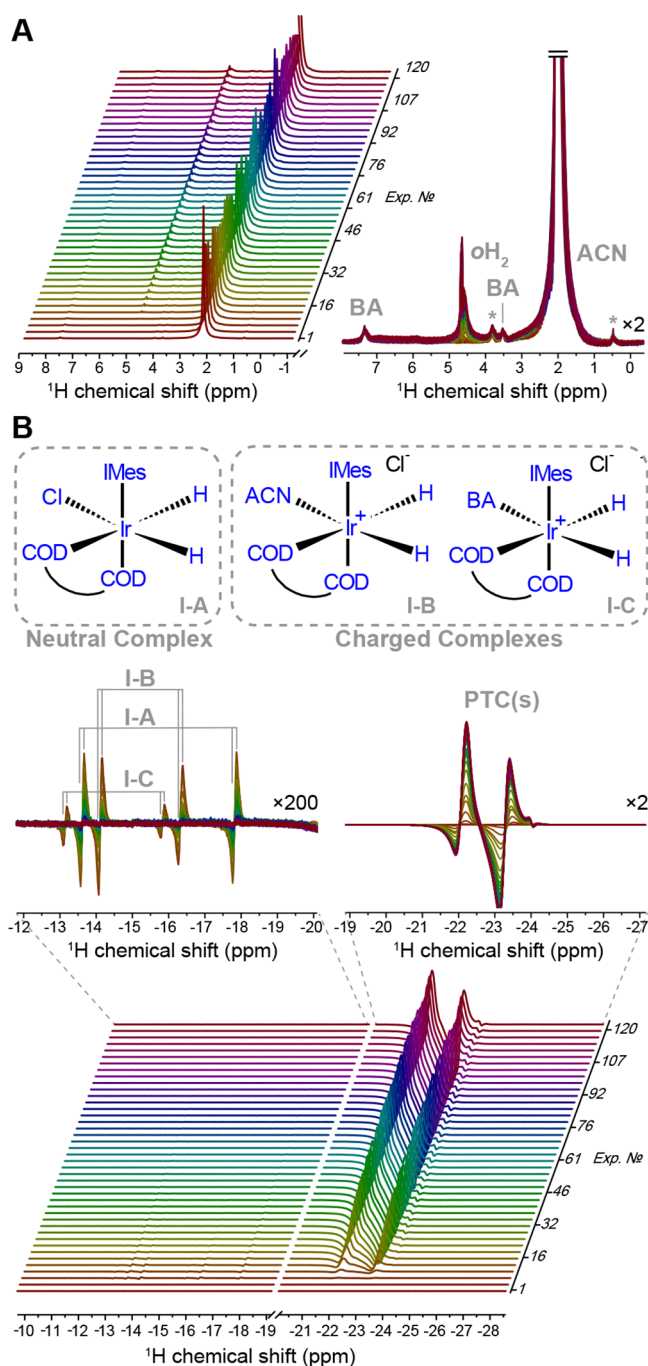


**Figure 1.** <sup>1</sup>H NMR spectra (1.1 T) of the SABRE solution following the catalyst activation process. The experimental sequence consisted of 3 s intervals of *p*H<sub>2</sub> bubbling (flow rates of 20 sccm at 6 bar), followed by 0.5 s of sample equilibration, and 16.5 s of resting which included <sup>1</sup>H NMR detection (single-scan, 45° excitation pulse, 6.5 s acquisition time). (A) Typical proton region of spectra displaying signals of benzylamine (BA) coligand, orthohydrogen (*o*H<sub>2</sub>), acetonitrile (ACN) solvent with <sup>13</sup>C-satellites denoted with asterisks. (B) Proposed chemical structures of neutral (I-A) and charged (I-B and I-C) intermediates observed in the hydride region (–12 to –27 ppm), our notation indicates that only one COD ligand is attached to Ir; polarization transfer catalysts (PTCs) are represented by peaks centered approximately –23 ppm.

equatorial double bond of the COD ligand and another one trans to the BA or ACN ligand in the equatorial plane of the Ir-complexes. One appears at –13 to –15 ppm (trans to COD),

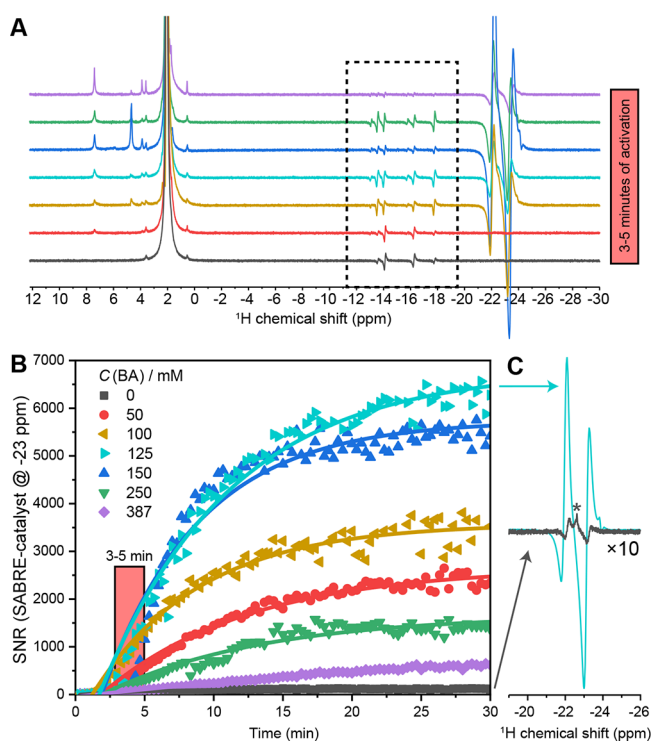


**Figure 2.** (A) <sup>1</sup>H benchtop (1.1 T) NMR spectra recorded in situ (single-scan, 45° excitation pulse) during the first 3–5 min of SABRE activation in the acetonitrile solvent; concentrations of coligand benzylamine (BA) and C(BA) were 0, 50, 125, 150, 175, 250, and 387 mM indicated by color. (B) Signal-to-noise ratio (SNR) for SABRE-catalysts (NMR peak at around -23 ppm) during the catalyst activation process. Each data point was collected every 20 s. (C) <sup>1</sup>H NMR of the PTC region after 30 min of activation with hydrogen, indicating the presence of neutral complexes [Ir(IMes)(H)<sub>2</sub>(ACN)<sub>2</sub>Cl], [Ir(IMes)(H)<sub>2</sub>(ACN)(BA)Cl], and [Ir(IMes)(H)<sub>2</sub>(BA)<sub>2</sub>Cl] (cyan, C(BA) = 125 mM) and a mixture of neutral [Ir(IMes)(H)<sub>2</sub>(ACN)<sub>2</sub>Cl] complexes and a symmetric charged [Ir(IMes)(H)<sub>2</sub>(ACN)<sub>3</sub>]Cl complex (gray, C(BA) = 0 mM).

and another at -15 to -18 ppm (trans to BA, ACN, or chlorine). The intermediate I-A is assigned to a neutral intermediate that shows NMR signals at -17.94 ppm (<sup>1</sup>H trans to chlorine) and -13.70 ppm (<sup>1</sup>H trans to COD). This intermediate has been elucidated in detail by Tickner et al.,<sup>24,26</sup>

c.f. Table 1 lists <sup>1</sup>H NMR chemical shifts, which are in agreement with assignments presented in this work. The charged intermediate I-B shows signals at -16.39 ppm (<sup>1</sup>H trans to ACN) and -14.19 ppm (<sup>1</sup>H trans to COD), and the second charged intermediate I-C at -15.91 ppm (<sup>1</sup>H trans to BA) and -13.22 ppm (<sup>1</sup>H trans to COD). The neutral intermediate predominates in nonpolar solvents, for example dichloromethane (DCM) used in this work, where the solvation of charged Ir-dihydride complexes and the chlorine counterion is unfavorable. In contrast, polar solvents like methanol (MeOH) solvate predominantly charged Ir-dihydride complexes. Acetonitrile, whose polarity lies between that of MeOH and DCM, can solvate both neutral and charged intermediates and PTCs.

After the start of the elucidated activation process, intermediate Ir-dihydride complexes generated are distributed across both pathways. At this point, a variety of complexes coexist in the SABRE system and the generation of several PTCs is conceivable, including both charged and neutral configurations. DFT calculations could give preliminary understanding of the stability of the individual Ir-dihydride complexes, although this exceeds the scope of the current work. The assignment presented was further analyzed in a series of dilution experiments with Co-L benzylamine, where <sup>1</sup>H benchtop NMR spectra of individual samples with their maximum SNR for Ir-dihydride complexes were recorded after 3 to 5 min of activation with hydrogen, cf. stacking <sup>1</sup>H NMR spectra shown in Figure 2A.

Generation of Ir-dihydride complexes was observed for all studied samples, however, NMR signals from PTCs were moderate for acetonitrile solvent without stabilizing Co-L, and for acetonitrile solvent with high concentrations of Co-L (C(BA) ≥ 250 mM, C([Ir]) = 5 mM), see Figure 2B,C. Highest <sup>1</sup>H SNR of Ir-dihydride PTCs was observed for samples with intermediate Co-L concentration (125 mM). Compared to ACN, BA shows a much slower exchange dynamic,<sup>27,30</sup> so that available Co-L first leads to additional stability and lifetime of mixed PTCs with ACN and then blocks the ligand positions at high concentrations.<sup>34</sup> The <sup>1</sup>H NMR spectra were acquired over a period of around 6 s, covering the time scales of most exchange pathways of substrate and pH<sub>2</sub>.

**Table 1.** <sup>1</sup>H Chemical Shifts δ(R-Ir(IMes)(COD)-H) of Intermediate Ir-Dihydride Complexes, with R Being Bound Ligands: Acetonitrile, Ammonia, Chlorine, or Benzylamine Generated by Activation of [Ir(IMes)(COD)Cl] with Hydrogen in Acetonitrile (ACN), Dichloromethane (DCM), and Methanol (MeOH)<sup>a</sup>

reference	R	solvent	available ligands	δ(COD-Ir-H)/ppm	δ(R-Ir-H)/ppm	Δ[δ(COD-Ir-H) - δ(R-Ir-H)]/ppm
this work	ACN	ACN (1.94 ppm)	ACN, Cl	-14.26	-16.38	2.13
	Cl			-13.72	-17.92	4.20
	Cl	ACN (1.94 ppm)	ACN, BA, Cl	-13.70	-17.94	4.24
	ACN			-14.19	-16.39	2.20
	BA			-13.22	-15.91	2.70
	Cl	DCM (5.32 ppm)	BA, Cl	-13.64	-17.96	4.32
	NH <sub>3</sub>	DCM extract (5.32 ppm)	NH <sub>3</sub> , Cl	-13.08	-15.41, -15.70( <sup>15</sup> N)	2.47
	Cl			-13.67	-18.10	4.42
	NH <sub>3</sub>	MeOH(3.31 ppm)	NH <sub>3</sub> , Cl	-13.22	-15.26, -15.56( <sup>15</sup> N)	2.19
	Tickner et al. <sup>24</sup>	Cl	CDCl <sub>3</sub>	DMSO	-13.39	-18.42
Tickner et al. <sup>26</sup>	Cl	CD <sub>2</sub> Cl <sub>2</sub>		-13.43	-18.04	4.61

<sup>a</sup><sup>1</sup>H NMR data recorded in situ at 46.7 MHz using 45° pulse excitation.

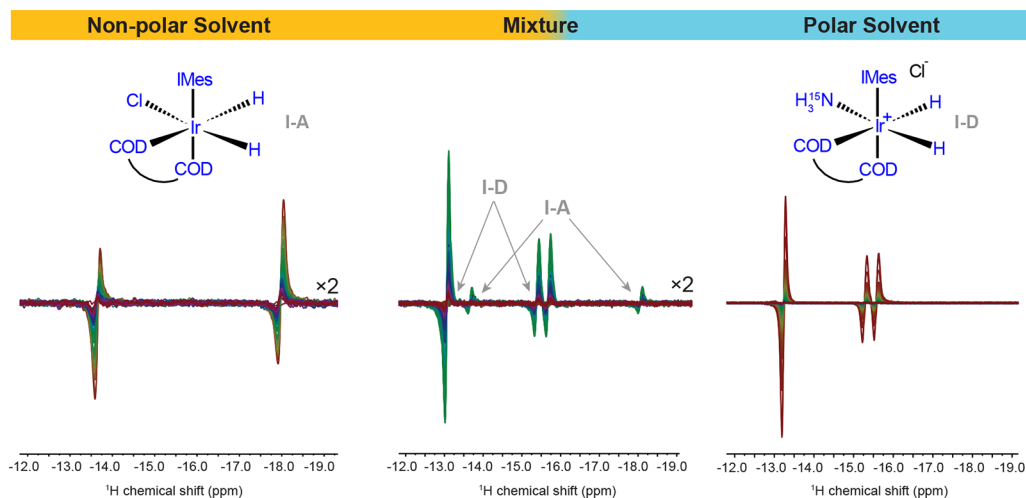


**Figure 3.**  $^1\text{H}$  NMR spectra (single-scan,  $45^\circ$  excitation pulse) of SABRE solutions containing  $^{15}\text{N}$ -labeled substrates. Nonpolar solvent: dichloromethane (DCM), 100 mM [ $^{15}\text{N}$ ]-benzylamine (BA) and 5 mM Ir(COD)(IMes)Cl; mixture: extraction of  $\text{NH}_3$  from 14 M aqueous solution into DCM with 3 mM Ir(COD)(IMes)Cl, spectrum of the DCM phase which contains around 0.2% of  $\text{H}_2\text{O}$ ; polar solvent: 60 mM  $^{15}\text{N}$ -ammonia in methanol) following the catalyst activation process. Spectra show the presence of a neutral intermediate (I-A) and charged complex with ammonia (I-D).

Figure 2B shows the results for the signal-to-noise ratio (SNR) of observed PTCs during activation monitoring. Presented values were calculated from a broad range of chemical shifts ( $-20$  to  $-26$  ppm, centered around the PTC signals) so that several active Ir-dihydride complexes were taken into account. Interestingly, another PTC signal in the  $-24$  ppm range (small sharp resonance on the right shoulder of the main peak) was detected at higher concentrations of BA, see Figure 2C. The complexity of the observed  $^1\text{H}$  NMR multiplets corresponding to PTCs means that observable signal enhancement in the SABRE process is a result of the interplay between the action of a variety of PTCs. Complexes present in low concentrations could still contribute significantly to the enhanced signal through efficient hyperpolarization through their unique  $J$ -coupling topology, chemical exchange dynamics, and lifetime.<sup>25</sup> In the following, the generation of neutral and charged Ir-dihydride complexes and the direction of the activation pathways dependent on solvent polarity is studied in detail.

Figure 3 shows a superimposed time series of  $^1\text{H}$  NMR spectra that illustrate the activation data of  $^{15}\text{N}$ -BA in DCM,  $^{15}\text{N}$ -ammonia in a DCM/water mixture, and  $^{15}\text{N}$ -ammonia in methanol using the precursor complex [Ir(COD)(IMes)Cl]. In DCM, intermediate I-A exhibits NMR signals at  $-17.96$  ppm ( $^1\text{H}$  trans to chlorine) and  $-13.64$  ppm ( $^1\text{H}$  trans to COD), indicating a slight increase in the inequivalence of these protons compared to the solvent ACN. For this intermediate, the choice of substrate does not play a significant role in influencing the detected  $^1\text{H}$  NMR signals because the substrate is absent in the neutral intermediate; however, variations of an overall proton concentration in the system might substantially affect speciation.<sup>35</sup> Furthermore, experiments with BA enriched with  $^{15}\text{N}$  provide additional evidence that the neutral intermediate is generated primarily in DCM. If BA were binding, as required for the charged intermediate, splitting of the Ir-dihydride signal via trans-coupling to the  $^{15}\text{N}$ -labeled BA would be expected. However, no such splitting was observed, indicating that the charged intermediate is not favored under these conditions. In contrast,  $^1\text{H}$  coupled to  $^{15}\text{N}$  for intermediate Ir-dihydride complexes was observed with the

substrate  $^{15}\text{N}$ -ammonia in the mixture of DCM with around 0.2% water (sample was prepared by extraction of  $\text{NH}_3/\text{NH}_4\text{OH}$  of 14 M aqueous solution into DCM), and for  $^{15}\text{N}$ -ammonia in methanol, c.f. Figure 3 and Table 1. The charged complex I-D shows split NMR signals at  $-15.26$  ppm and  $-15.56$  ( $^1\text{H}$  trans to  $^{15}\text{N}$ -ammonia) and a signal at  $-13.22$  ppm ( $^1\text{H}$  trans to COD). For the mixture, I-D shows NMR signals at  $-15.41$  ppm and  $-15.70$  ( $^1\text{H}$  trans to  $^{15}\text{N}$ -ammonia) and  $-13.08$  ppm ( $^1\text{H}$  trans to COD). In addition, a second pair of signals from a neutral complex I-A at  $-18.10$  ppm ( $^1\text{H}$  trans to chlorine) and  $-13.67$  ppm ( $^1\text{H}$  trans to COD) is observed. Multiplet structure of the peaks corresponding to intermediates in principle allows extracting proton–proton  $J$ -coupling values, and they lie within  $-4$  to  $-7$  Hz range, see Table 1. Although the majority of the mixture consists of nonpolar DCM, signals from the charged complexes are dominant.

In summary, a generalized trend can be identified with the SABRE systems examined in this study: intermediate Ir-dihydride complexes and polarization transfer catalysts in SABRE-based hyperpolarization exhibit at least two different forms, one being a charged and a second being a neutral configuration, and generation of these Ir-dihydride complexes can be controlled by the polarity of the solvent. This understanding provides a valuable foundation for designing the chemical composition of solvent–SABRE mixtures. The ability to efficiently polarize solvent molecules themselves is important in various fundamental physics experiments, where generating large volumes of highly polarized substances remains a critical challenge.<sup>36,37</sup>

## CONCLUSIONS

Using benchtop  $^1\text{H}$  NMR spectroscopy in combination with an in situ hyperpolarization technique based on  $p\text{H}_2$ , we investigated an activation process of a typical SABRE catalyst precursor [Ir(COD)(IMes)Cl]. A protocol for obtaining stable and long-lasting hyperpolarization of acetonitrile in the presence of benzylamine as a stabilizing coligand was successfully established.

Our findings show simultaneous generation of charged and neutral Ir-dihydride complexes during the activation of the Ir-precursor with  $p\text{H}_2$  in acetonitrile solvent. This was further investigated in common solvents used for SABRE hyperpolarization, where neutral Ir-dihydride complexes were predominantly observed in nonpolar solvents (e.g., dichloromethane), charged Ir-dihydride complexes – in polar solvents (e.g., methanol), and both configurations – in dichloromethane/water mixtures. These results demonstrate that complex speciation is affected by solvent polarity, offering a generalized understanding for polarizing various solvents with SABRE. The polarity of acetonitrile is somewhere between that of MeOH and DCM, where both neutral and charged Ir-dihydride complexes were assigned.

Furthermore, this study highlights the broader implications of SABRE for fundamental physics experiments requiring large volumes of hyperpolarized molecules. The established protocol provides a reliable methodology for acetonitrile solvent polarization and opens new possibilities for generating effective polarization transfer catalysts in other conditions, potentially extending to complex systems such as emulsions. Future work could explore the role of exchange dynamics,  $J$ -coupling topologies, and solvent interactions to further enhance polarization efficiency and stability.

## ■ ASSOCIATED CONTENT

### Data Availability Statement

Raw data is available online: <https://doi.org/10.6084/m9.figshare.29118959.v1>.

### SI Supporting Information

The Supporting Information is available free of charge at <https://pubs.acs.org/doi/10.1021/acs.organomet.5c00052>.

Solvent hyperpolarization of acetonitrile, chemicals, experimental setup and methods, Ir-dihydride intermediates in the transformation of PTCs, hyperpolarization of  $^{15}\text{N}$ -acetonitrile (PDF)

## ■ AUTHOR INFORMATION

### Corresponding Author

**Danila A. Barskiy** – Johannes Gutenberg Universität Mainz, 55128 Mainz, Germany; Helmholtz-Institut Mainz, 55128 Mainz, Germany; Helmholtzzentrum für Schwerionenforschung, 64291 Darmstadt, Germany; [orcid.org/0000-0002-2819-7584](https://orcid.org/0000-0002-2819-7584); Email: [dbarskiy@uni-mainz.de](mailto:dbarskiy@uni-mainz.de)

### Authors

**Raphael Kircher** – Johannes Gutenberg Universität Mainz, 55128 Mainz, Germany; Helmholtz-Institut Mainz, 55128 Mainz, Germany; Helmholtzzentrum für Schwerionenforschung, 64291 Darmstadt, Germany; [orcid.org/0000-0002-7980-7995](https://orcid.org/0000-0002-7980-7995)

**Jingyan Xu** – Johannes Gutenberg Universität Mainz, 55128 Mainz, Germany; Helmholtz-Institut Mainz, 55128 Mainz, Germany; Helmholtzzentrum für Schwerionenforschung, 64291 Darmstadt, Germany; [orcid.org/0000-0003-0688-5404](https://orcid.org/0000-0003-0688-5404)

**Erik van Dyke** – Johannes Gutenberg Universität Mainz, 55128 Mainz, Germany; Helmholtz-Institut Mainz, 55128 Mainz, Germany; Helmholtzzentrum für Schwerionenforschung, 64291 Darmstadt, Germany

**Rozana Mazlumian** – Cavendish Laboratory, University of Cambridge, Cambridge CB3 0HE, U.K.

**Dmitry Budker** – Johannes Gutenberg Universität Mainz, 55128 Mainz, Germany; Helmholtz-Institut Mainz, 55128 Mainz, Germany; Helmholtzzentrum für Schwerionenforschung, 64291 Darmstadt, Germany; Department of Physics, UC Berkeley, Berkeley, California 94720-1234, United States

Complete contact information is available at:

<https://pubs.acs.org/10.1021/acs.organomet.5c00052>

## Funding

Alexander von Humboldt Foundation in the framework of the Sofja Kovalevskaja Award.

## Notes

The authors declare no competing financial interest.

## ■ ACKNOWLEDGMENTS

We acknowledge Prof. Simon Duckett, Prof. Igor Koptyug, and Dr. Kerstin Münnemann for stimulating discussions. The publication is funded by the Open Access Publishing Fund of GSI Helmholtzzentrum für Schwerionenforschung.

## ■ REFERENCES

- (1) van Beek, T. A. Low-field benchtop NMR spectroscopy: status and prospects in natural product analysis. *Phytochem. Anal.* **2021**, *32*, 24–37.
- (2) Singh, K.; Blümich, B. NMR spectroscopy with compact instruments. *Trends Anal. Chem.* **2016**, *83*, 12–26.
- (3) Blümich, B. Introduction to compact NMR: A review of methods. *Trends Anal. Chem.* **2016**, *83*, 2–11.
- (4) Kircher, R.; Hasse, H.; Münnemann, K. High Flow-Rate Benchtop NMR Spectroscopy Enabled by Continuous Overhauser DNP. *Anal. Chem.* **2021**, *93*, 8897–8905.
- (5) Giraudeau, P.; Felpin, F.-X. Flow reactors integrated with in-line monitoring using benchtop NMR spectroscopy. *React. Chem. Eng.* **2018**, *3*, 399–413.
- (6) Bouillaud, D.; Farjon, J.; Gonçalves, O.; Giraudeau, P. Benchtop NMR for the monitoring of bioprocesses. *Magn. Reson. Chem.* **2019**, *57*, 794–804.
- (7) Castaing-Cordier, T.; Bouillaud, D.; Farjon, J.; Giraudeau, P. Recent advances in benchtop NMR spectroscopy and its applications. **2021**, *103*, 191–258.
- (8) Wu, H.; Wang, Y.; Shi, Z.; Wang, X.; Yang, J.; Xiao, M.; Ge, J.; Xing, W.; Liu, C. Recent developments of iridium-based catalysts for the oxygen evolution reaction in acidic water electrolysis. *J. Mater. Chem. A* **2022**, *10*, 13170–13189.
- (9) Timofeeva, D. S.; Lindsay, D. M.; Kerr, W. J.; Nelson, D. J. Are rate and selectivity correlated in iridium-catalysed hydrogen isotope exchange reactions? *Catal. Sci. Technol.* **2021**, *11*, 5498–5504.
- (10) Kerr, W. J.; Reid, M.; Tuttle, T. Iridium-Catalyzed C–H Activation and Deuteration of Primary Sulfonamides: An Experimental and Computational Study. *ACS Catal.* **2015**, *5*, 402–410.
- (11) Cui, C.-X.; Chen, H.; Li, S.-J.; Zhang, T.; Qu, L.-B.; Lan, Y. Mechanism of Ir-catalyzed hydrogenation: A theoretical view. *Coord. Chem. Rev.* **2020**, *412*, No. 213251.
- (12) Adams, R. W.; Aguilar, J. A.; Atkinson, K. D.; Cowley, M. J.; Elliott, P. I. P.; Duckett, S. B.; Green, G. G. R.; Khazal, I. G.; López-Serrano, J.; Williamson, D. C. Reversible Interactions with Parahydrogen Enhance NMR Sensitivity by Polarization Transfer. *Science* **2009**, *323*, 1708–1711.
- (13) Atkinson, K. D.; Cowley, M. J.; Elliott, P. I. P.; Duckett, S. B.; Green, G. G. R.; López-Serrano, J.; Whitwood, A. C. Spontaneous Transfer of Parahydrogen Derived Spin Order to Pyridine at Low Magnetic Field. *J. Am. Chem. Soc.* **2009**, *131*, 13362–13368.

- (14) Pravdivtsev, A. N.; Ivanov, K. L.; Yurkovskaya, A. V.; Petrov, P. A.; Limbach, H.-H.; Kaptein, R.; Vieth, H.-M. Spin polarization transfer mechanisms of SABRE: A magnetic field dependent study. *J. Magn. Reson.* **2015**, *261*, 73–82.
- (15) Rayner, P. J.; Gillions, J. P.; Hannibal, V. D.; John, R. O.; Duckett, S. B. Hyperpolarisation of weakly binding N-heterocycles using signal amplification by reversible exchange. *Chem. Sci.* **2021**, *12*, 5910–5917.
- (16) Sellies, L.; Reile, I.; Aspers, R. L. E. G.; Feiters, M. C.; Rutjes, F. P. J. T.; Tessari, M. Parahydrogen induced hyperpolarization provides a tool for NMR metabolomics at nanomolar concentrations. *Chem. Commun.* **2019**, *55*, 7235–7238.
- (17) Reile, I.; Eshuis, N.; Hermkens, N. K. J.; van Weerdenburg, B. J. A.; Feiters, M. C.; Rutjes, F. P. J. T.; Tessari, M. NMR detection in biofluid extracts at sub- $\mu\text{M}$  concentrations via para- $\text{H}_2$  induced hyperpolarization. *Analyst* **2016**, *141*, 4001–4005.
- (18) Kircher, R.; Mross, S.; Hasse, H.; Münnemann, K. Functionalized Controlled Porous Glasses for Producing Radical-Free Hyperpolarized Liquids by Overhauser DNP. *Molecules* **2022**, *27*, 6402.
- (19) Silva Terra, A. I.; Taylor, D. A.; Halse, M. E. Hyperpolarised benchtop NMR spectroscopy for analytical applications. *Prog. Nucl. Magn. Reson. Spectrosc.* **2024**, *144–145*, 153–178.
- (20) Bütikofer, M.; Stadler, G. R.; Torres, F. Rescaling NMR for a Larger Deployment in Drug Discovery: Hyperpolarization and Benchtop NMR as Potential Game-Changers. *Chemistry Methods* **2024**, *4*, e202400009.
- (21) Rayner, P. J.; Richardson, P. M.; Duckett, S. B. The Detection and Reactivity of Silanols and Silanes Using Hyperpolarized  $^{29}\text{Si}$  Nuclear Magnetic Resonance. *Angew. Chem., Int. Ed.* **2020**, *59*, 2710–2714.
- (22) Tickner, B. J.; Ahwal, F.; Whitwood, A. C.; Duckett, S. B. Reversible Hyperpolarization of Ketoisocaproate Using Sulfoxide-containing Polarization Transfer Catalysts. *ChemPhysChem* **2021**, *22*, 13–17.
- (23) Kircher, R.; Xu, J.; Barskiy, D. A. In Situ Hyperpolarization Enables  $^{15}\text{N}$  and  $^{13}\text{C}$  Benchtop NMR at Natural Isotopic Abundance. *J. Am. Chem. Soc.* **2024**, *146*, 514–520.
- (24) Tickner, B. J.; Lewis, J. S.; John, R. O.; Whitwood, A. C.; Duckett, S. B. Mechanistic insight into novel sulfoxide containing SABRE polarisation transfer catalysts. *Dalton Transact.* **2019**, *48*, 15198–15206.
- (25) Knecht, S.; Hadjiali, S.; Barskiy, D. A.; Pines, A.; Sauer, G.; Kiryutin, A. S.; Ivanov, K. L.; Yurkovskaya, A. V.; Buntkowsky, G. Indirect Detection of Short-Lived Hydride Intermediates of Iridium N-Heterocyclic Carbene Complexes via Chemical Exchange Saturation Transfer Spectroscopy. *J. Phys. Chem. C* **2019**, *123*, 16288–16293.
- (26) Tickner, B. J.; Dennington, M.; Collins, B. G.; Gater, C. A.; Tanner, T. F. N.; Whitwood, A. C.; Rayner, P. J.; Watts, D. P.; Duckett, S. B. Metal-Mediated Catalytic Polarization Transfer from para Hydrogen to 3,5-Dihalogenated Pyridines. *ACS Catal.* **2024**, *14*, 994–1004.
- (27) Mewis, R. E.; Green, R. A.; Cockett, M. C. R.; Cowley, M. J.; Duckett, S. B.; Green, G. G. R.; John, R. O.; Rayner, P. J.; Williamson, D. C. Strategies for the Hyperpolarization of Acetonitrile and Related Ligands by SABRE. *J. Phys. Chem. B* **2015**, *119*, 1416–1424.
- (28) Tickner, B. J.; Duckett, S. B. Iridium trihydride and tetrahydride complexes and their role in catalytic polarisation transfer from parahydrogen to pyruvate. *Chem. Sci.* **2025**, *16*, 1396–1404.
- (29) Truong, M. L.; Theis, T.; Coffey, A. M.; Shchepin, R. V.; Waddell, K. W.; Shi, F.; Goodson, B. M.; Warren, W. S.; Chekmenev, E. Y.  $^{15}\text{N}$  hyperpolarization by reversible exchange using SABRE-SHEATH. *J. Phys. Chem. C* **2015**, *119*, 8786–8797.
- (30) Fekete, M.; Ahwal, F.; Duckett, S. B. Remarkable Levels of  $^{15}\text{N}$  Polarization Delivered through SABRE into Unlabeled Pyridine, Pyrazine, or Metronidazole Enable Single Scan NMR Quantification at the mM Level. *J. Phys. Chem. B* **2020**, *124*, 4573–4580.
- (31) Sheberstov, K.; Van Dyke, E.; Xu, J.; Kircher, R.; Chuchkova, L.; Hu, Y.; Alvi, S.; Budker, D.; Barskiy, D. A. Robotic arms for hyperpolarization-enhanced NMR. *JMRO* **2025**, *23*, No. 100194.
- (32) Bowers, C. R.; Weitekamp, D. P. Transformation of Symmetrization Order to Nuclear-Spin Magnetization by Chemical Reaction and Nuclear Magnetic Resonance. *Phys. Rev. Lett.* **1986**, *57*, 2645–2648.
- (33) Bowers, C. R.; Weitekamp, D. P. Parahydrogen and synthesis allow dramatically enhanced nuclear alignment. *J. Am. Chem. Soc.* **1987**, *109*, 5541–5542.
- (34) Barskiy, D.; Pravdivtsev, A.; Ivanov, K.; Kovtunov, K.; Koptuyug, I. A simple analytical model for signal amplification by reversible exchange (SABRE) process. *Phys. Chem. Chem. Phys.* **2016**, *18*, 89–93.
- (35) Olaru, A. M.; Burns, M. J.; Green, G. G. R.; Duckett, S. B. SABRE hyperpolarisation of vitamin B3 as a function of pH. *Chem. Sci.* **2017**, *8*, 2257–2266.
- (36) Dagys, L.; Korzeczek, M. C.; Parker, A. J.; Eills, J.; Blanchard, J. W.; Bengs, C.; Levitt, M. H.; Knecht, S.; Schwartz, I.; Plenio, M. B. Robust parahydrogen-induced polarization at high concentrations. *Sci. Adv.* **2024**, *10*.
- (37) Vaneeckhaute, E.; Tyburn, J.-M.; Kempf, J. G.; Martens, J. A.; Breynaert, E. Identifying routes for transferring spin polarization from parahydrogen to protic solvents. *Chem. Commun.* **2024**, *60*, 13923–13926.



CAS BIOFINDER DISCOVERY PLATFORM™

**PRECISION DATA  
FOR FASTER  
DRUG  
DISCOVERY**

CAS BioFinder helps you identify targets, biomarkers, and pathways

**Unlock insights**

CAS  
A Division of the  
American Chemical Society